NRIAG JOURNAL OF ASTRONOMY AND GEOPHYSICS
2020, VOL. 9, NO. 1, 433–448
https://doi.org/10.1080/20909977.2020.1761134

Immediate settlement of footing using interpreted seismic refraction geoelastic data: a case study of Eket county, Nigeria

Joseph Gordian Atat[a], Nyakno Jimmy George[b] and Anthonia Gordian Atat[c]

[a]Department of Physics, University of Uyo, Uyo, Nigeria; [b]Department of Physics, Geophysics Research Group (GRG), Akwa Ibom State University, Nigeria; [c]Department of Geology and Mineral Sciences, University of Ilorin, Ilorin, Nigeria

ABSTRACT

Immediate settlement of footing was assessed at five different locations in Eket using known parameters (measured and calculated) that were obtained from the interpretation of 12 channel digital type signal enhancement seismograph (Terraloc Mark Six). Results obtained show that immediate settlement of footing is approximately 0.025 m in all the locations. This was determined at width B $<$ 20 ft (6.096 m). The boundary condition (limit) for bearing pressure in the area by this study falls within the range of 1694 psf (or 81,131 Pa) $\leq q \leq$ 29934psf (or 143,380 Pa). The class of materials in the area (first layer) falls under row five and row six, column one of International Residential Code, 2006. The study reveals that the area has a threshold subgrade coefficient of 29,298 Nm^{-3} while the descent of footing under load per metre is 159.7. These parameters further characterise the foundation under load in the study area.

ARTICLE HISTORY
Received 13 June 2019
Revised 15 April 2020
Accepted 18 April 2020

KEYWORDS
Immediate settlement; footing; bearing pressure; seismic refraction and data; NAVFAC

1. Introduction

Shallow foundations are designed to satisfy bearing capacity and settlement limit criteria. Settlement limit criteria generally control the design of foundation on cohesion and cohesionless soils, and is more critical than bearing capacity failure that settlement is expected to be within tolerable limits. The selection of foundation system for highway bridges and others involve the consideration of performance and cost. For adequate performance, the foundation must satisfy the bearing capacity requirements to support the piers, abutments, and superstructure and must satisfy the settlement limits. In shallow foundation, spread footings consist of strips or a pad of concrete (or other material) which extends below the frost line and transfer the building loads to the underlying soil or rock. Another type of shallow footing is the slab-on -grade footing where the building loads are transferred to the soil through a concrete slab placed at the surface. A deep footing is an engineered structure used to transfer from structure to stronger deeper soil layers or bedrock.

Geotechnical testing has increasingly been used for geotechnical investigation to identify subsurface irregularities such as fill, cavities and variable strata (Fumal and Tinsley 1985; Budhu and Al-Karni 1993). It can also be used to obtain quantitative information that is useful for foundation assessment and design. This work uses the bearing capacity data obtained by Atat et al. (2013) which was based on the Allowable Bearing Capacity for Shallow Foundation in Eket. The combined use of compressional and shear wave velocities gives a better resolution of the quality of geomaterials in which they have propagated through (Sarma and Lossifelis 1990; Richards et al. 1993; Dormieux and Pecker 1995; Paolucci and Pecker 1997; Soubra 1997; Kumar and Kumar 2003). Rock elastic properties are sources of valuable information for most projects in rock mechanics as the knowledge of deformational characteristics of rocks is paramount in locating and extracting mineral resources and design and construction of any structure on the rock or soil.

Footings are typically designed in sandy soils such that the allowable settlement is less than 25 mm. Applied loads from the superstructure need to be safely recommended by the design and construction codes. Elastic or Immediate settlement in sandy soils is assumed to occur instantaneously when static loads are applied. Several equations are proposed to estimate the settlement of footings in sands as it can affect the bearing capacity of the soil. Settlement of foundation includes settlement under loads and settlement due to other causes. Foundation settlement under load can be classified into three types: Immediate or Elastic settlement (S_i) which takes place during or immediately after construction of the structure. It is also known as distortion settlement as it is due to distortions (and not the volume change) within the foundation soil. Although the settlement is not truly elastic, it is

CONTACT Nyakno Jimmy George nyaknojimmyg@gmail.com Department of Physics, Geophysics Research Group (GRG), Akwa Ibom State University, Nigeria

computed using elastic theory, especially for cohesive soils. Another is consolidation settlement (S_c) that occurs due to gradual expulsion of water from the void of the soil. This component is determined using Terzaghi's theory of consolidation. The third foundation settlement is secondary consolidation settlement (S_s). This component occurs after completion of the primary consolidation. The secondary consolidation is not significant for clay and silty soils. The total settlement (S) is given by

$$S = S_i + S_c + S_s \tag{1}$$

(Arora 2009).

Settlement due to other causes includes: the settlement which occurs due to underground erosion, structural collapse of soil, thermal changes, frost heave, vibration and shocks, mining subsidence, landslides, creep and changes in the vicinity.

The linear theory of elasticity is used to determine the elastic settlement of the footings on saturated clay (Arora 2009). The vertical settlement under a uniformly distributed flexible area evaluation may be achieved using Equation (2).

$$S_i = qB\left(\frac{1-\mu^2}{E_s}\right)I \tag{2}$$

q is uniformly distributed load

B is characteristic length of the loaded area

E_s is the modulus of elasticity of the soil

μ is the Poisson's ratio

I is the influence factor

Immediate settlement of cohesionless soils can be computed using NAVFAC method given by

$$S_i = \frac{4qB^2}{K_s(B+1)^2} \tag{3}$$

q is the bearing capacity

B is the width of the footing

K_s is the coefficient of subgrade

Soil is often treated as an elastic medium, linear or non-linear to which the elastic theory assumptions and principles of stress and strain are applied. Settlement computation of this form uses the elastic properties of Poisson's ratio and Young's modulus to represent the soil. A general expression for the elastic settlement relation is

$$S = \frac{qBI\sigma}{E} \tag{4}$$

There are three types of dry and partially saturated cohesionless soils. The first type comprises soils that consist essentially of small-sized to medium-sized grains of sufficient strength or under sufficiently small stresses so that grain breakage does not play a significant role in their behaviour. The second type includes those soils made up essentially of large-sized grains, such as rockfills. Large-sized grains may break under large stresses and overall volume changes are significantly conditioned by grain breakage. The third type includes fine-grained materials, such as silt. The behaviour of the first type of dry cohesionless soils can be described in terms of the void ratio. The behaviour of the second type depends on the normal stresses and grain size. If the water or air cannot escape at a sufficiently fast rate when the third type of soil is contracting due to vibration, significant pore pressure may develop, with the resulting liquefaction of the material. If pore water can flow in and out of the material at a sufficiently high rate so that appreciable pore pressures do not develop, behaviour of these soils does not differ qualitatively from that of partially saturated cohesionless soils. If the pore water cannot flow in and out of the material, cyclic loads will usually generate increased pore pressure. If the soil is loose or contractive, the soil may liquefy (NAVFAC 1997).

For safe design, the net footing pressure should be equal to or less than the net allowable bearing pressure ($q_n \leq q_{na}$). Immediate settlement of isolated shallow footings for $B < 20$ ft and $B > 40$ ft is, respectively, given in Equations (3) and (5) (Resin and Kasktas 2009; Birid and Chachar 2016).

$$S_i = \frac{2qB^2}{K_s(B+1)^2} \tag{5}$$

Foundation Footings: Code Basics, depth and width of footing in undisturbed soil should extend to a minimum of 12 and 12 ft, respectively. Other parameters relate with immediate settlement of footing explicitly or implicitly as given in Equations (6) and (11).

$$E = 2\mu(1+\sigma) \tag{6}$$

σ is Poisson's ratio

$$\sigma = \frac{\left(\frac{V_p}{V_s}\right)^2 - 2}{2\left(\left(\frac{V_p}{V_s}\right)^2 - 1\right)} \tag{7}$$

$$K = \frac{2\mu(1+\sigma)}{3(1-2\sigma)} \tag{8}$$

K is Bulk modulus

μ is Shear modulus

$$q_f = \frac{K_s}{40}$$

For shallow foundation (Terzaghi and Peck 1967).

$$q_a = \frac{q_f}{n} \tag{9}$$

$n = 4.0$ for soils called the factor of safety

q_f is the Ultimate Failure (Ultimate Bearing Capacity)

q_a is the safe/allowable bearing pressure

$$K_s = 4\gamma V_s \tag{10}$$

$$\gamma = \gamma_o + 0.002V_p \tag{11}$$

(Tezcan et al. 2009)

$\gamma_o = 16000Kgm^{-2}s^{-2}$ for loose, sandy and clayey soil (Tezcan et al. 2006).

What is needed in construction or foundation site is low compressibility and compliance and high bearing capacity (Scott et al. 1968). A foundation is shallow if its depth is equal to or less than its width. Footing is a foundation unit constructed in brickwork, masonry or concrete under the base of a wall or a column for the purpose of distributing the load over a large area. A footing or a shallow foundation is placed immediately below the lowest part of the superstructure supported it. Shallow foundations often called footings are usually embedded about a metre or so into the soil (Figure 1). Foundations are generally either shallow or deep (Terzaghi et al. 1996)

The minimum width of concrete or masonry footings for conventional light-frame construction is 12 inches for load-bearing value of soil in psf on first story. For the second story, the minimum width in inches is 15, 12, 12 and 12 for load-bearing values (psf) of 1500, 2000, 3000 and $\geq$ 4000, respectively. Also, the third story is given as 23, 17, 12 and 12, respectively, for the same load-bearing values. Table 1 relates the class of material to their corresponding load-bearing pressure.

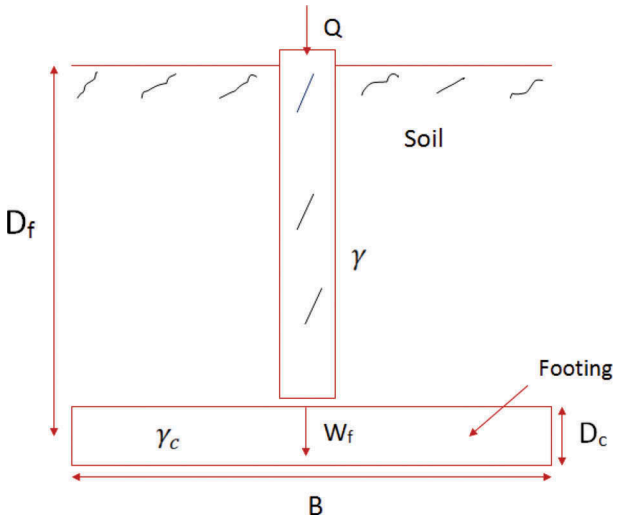

Figure 1. Foundation backfilled (Arora 2009).

Table 1. Loading pressure of materials [1 psf (Pounds per square foot) = 0.0479 kPa; 1 ft = 0.3048 m] (Internationl Residential Code 2006).

Class of Material	Load-Bearing Pressure (psf)
Crystalline bedrock	12,000
Sedimentary and foliated rock	6000
Sandy gravel and/or gravel	5000
Sand, silt sand, clayey, sand, silty gravel and clayey gravel	3000
Clay, Sandy clay, silty clay, clayey silt, silt and sandy silt	2000 and below

Q is the superimposed load
W_f is the weight of the footing and the soil above it
D_c is the thickness of footing
γ is the unit weight of soil
γ_c is the unit weight of concrete
The footing is laid at a shallow depth,$D_f \leq B$.

2. Site location and geology

The area of study (Eket in Akwa Ibom State, Nigeria) is located within latitudes 4°00′N to 4°30′N and longitudes 7°45′E to 8°00′E (Figure 2). Forest resources include timber, palm produce while the area is also noted for seafood production. Crops like yam, cassava, coco-yam, plantain to maize, vegetables and deposit of natural resources: crude oil and clay are present. The relief of Eket is relatively flat, though with some marshy river-washed soils around the banks of Qua Iboe River; it falls within the tropical zone wherein its dominant vegetation is the green foliage of trees/shrubs and the oil palm tree belt. Two seasons: the wet season and the dry season are experienced. The area is underlain by Sedimentary Formation of late Tertiary and Holocene ages geologically. The sea level from the surface is less than 176 m (Atat et al. 2013).

3. Materials and method

Some data defining elastic parameters, subgrade coefficient and bearing capacity (measured from seismic refraction data) were obtained from Atat et al. (2013) to extend the work by establishing a result that predicts immediate settlement of footing from seismic refraction data using NAVFAC method (NAVFAC 1982, 1997). The immediate settlement of footing was determined using Equation (3).

In the survey, seismic refraction testing was located along major/secondary roads in some parts of Eket, Akwa Ibom State, Nigeria. The spread line employed was 60 m based on 5 m geophone spacing. Using the above spread line and numerous shot points of the impact hammer, the depth observed was investigated by P and S waves propagated through different layers. Figure 3 shows some accessories used in generating seismic energy.

During data acquisition, individual shot records were displayed as variable area wiggle traces displaying travel time against distance (x). These enable an initial calculation of overburden and refractor apparent velocities and provide an important check on the quality of the data. The acquisition wiggle traces are used to display the data during picking of the first arrivals for each geophone position and shot (Figure 4). The processed data were presented as series of time-distance graphs where compressional and shear wave

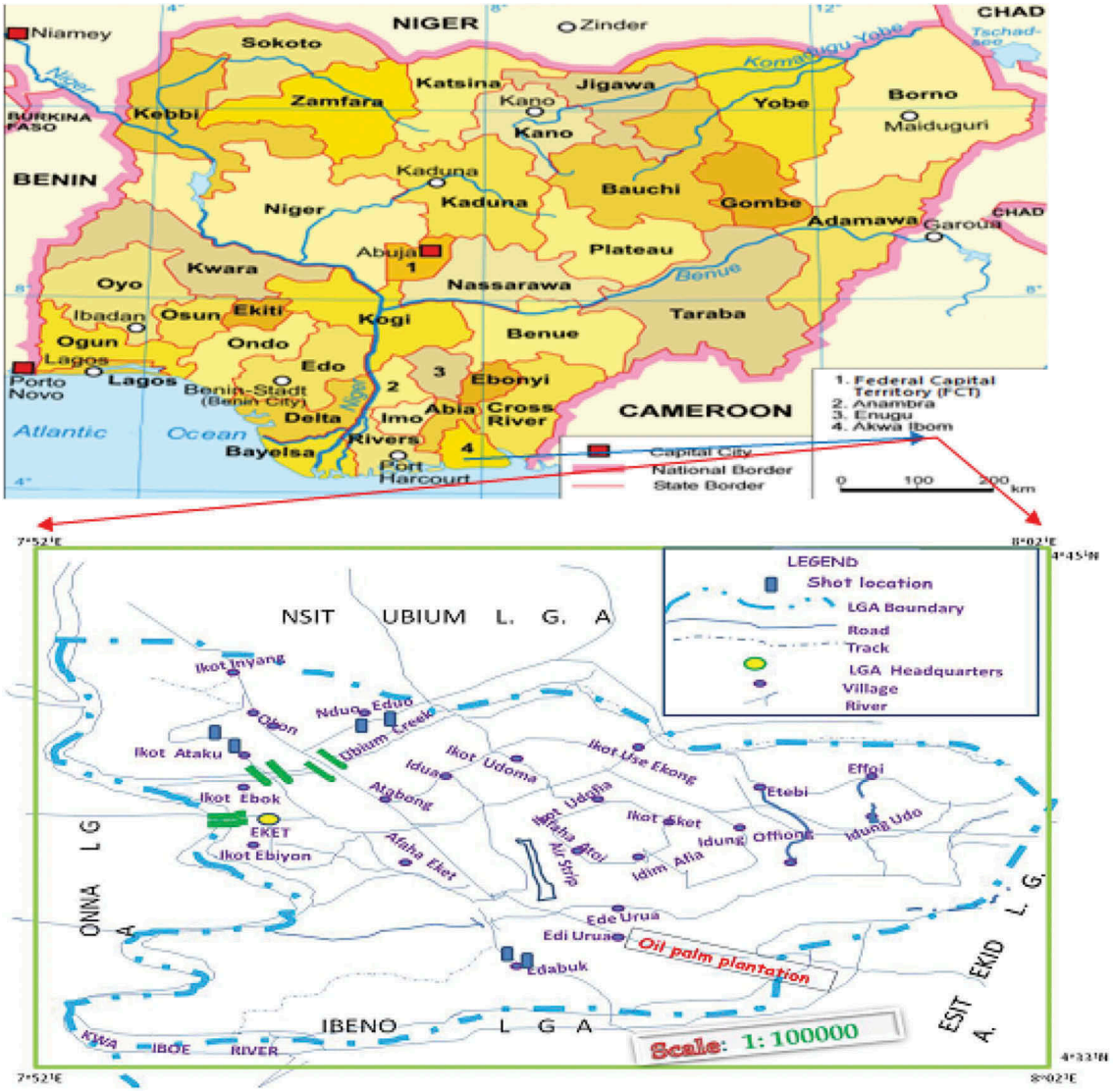

Figure 2. Map showing the location of Eket (the study area) in Akwa Ibom state (4) of Nigeria (Atat et al. 2013).

Figure 3. Some accessories used in field survey.

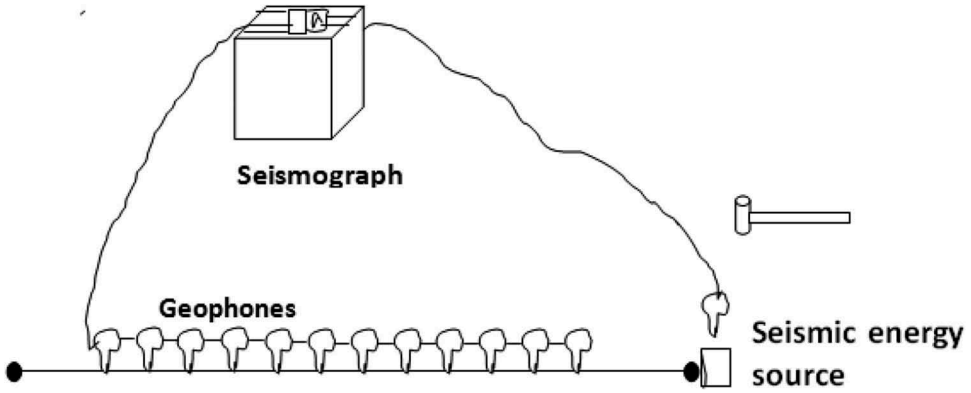

Figure 4. Schematic diagram of the detector geometry-field array.

velocities for each layer were obtained leading to the evaluation of coefficient of subgrade, bearing capacity and other parameters.

A seismic system consists of two sets of cable with a twelve channel spread cable for vertical geophones connected to the acquisition box on each side.

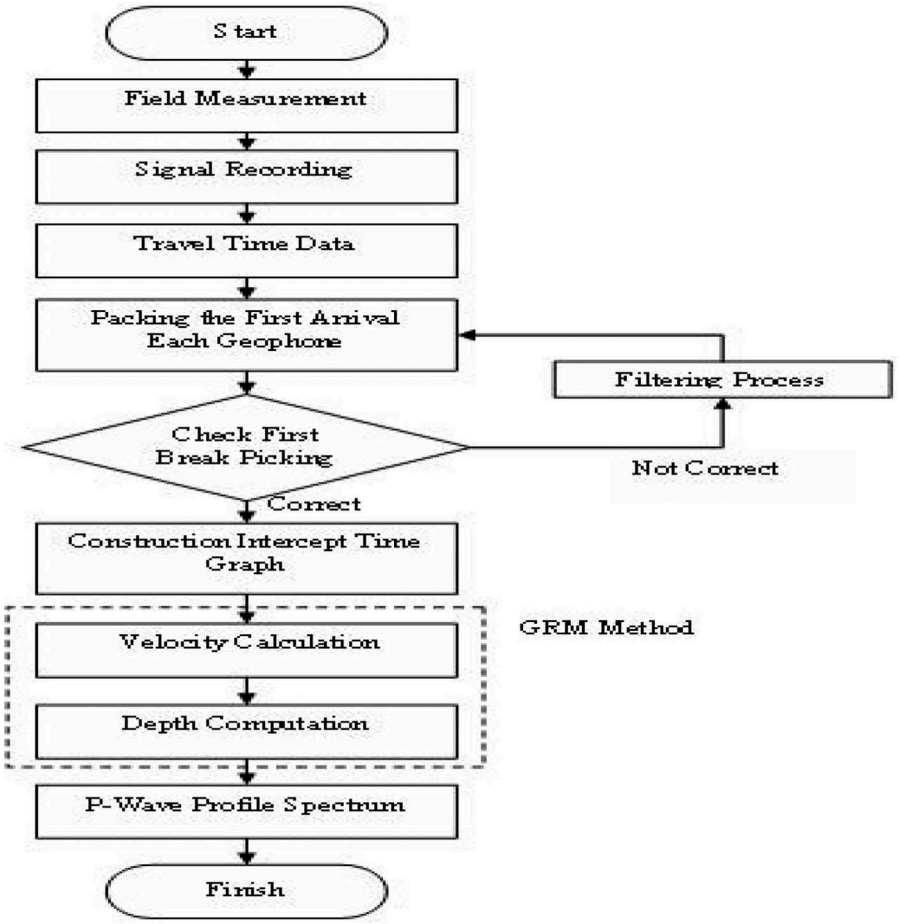

Figure 5. Data processing workflow.

Table 2. Summary of parameters estimation (B = 0.524).

S/N	Latitude (^{0}N)	Longitude (^{0}E)	q (N/m^2)	K_s (N/m^3)	B (m)	S_i (m)
1	4.6767	7.9256	143,380	22,940,000	0.524	0.025000872
2	4.6800	7.9303	114,560	18,330,000	0.524	0.024999454
3	4.6667	7.9147	81,131	13,010,000	0.524	0.024944197
4	4.6206	7.9325	83,560	13,370,000	0.524	0.024999252
5	4.6125	7.9419	89,190	14,270,000	0.524	0.025000701

Table 3. Summary of parameters estimation (B = 1.3716).

S/N	Latitude (^{0}N)	Longitude (^{0}E)	q (N/m^2)	K_s (N/m^3)	B (m)	S_i (m)
1	4.6767	7.9256	143,380	22,940,000	1.3716	0.025000872
2	4.6800	7.9303	114,560	18,330,000	1.3716	0.024999454
3	4.6667	7.9147	81,131	13,010,000	1.3716	0.024944197
4	4.6206	7.9325	83,560	13,370,000	1.3716	0.024999252
5	4.6125	7.9419	89,190	14,270,000	1.3716	0.025000701

Table 4. Summary of parameters estimation (B = 2.8956).

S/N	Latitude (^{0}N)	Longitude (^{0}E)	q (N/m^2)	K_s (N/m^3)	B (m)	S_i (m)
1	4.6767	7.9256	143,380	22,940,000	2.8956	0.025000872
2	4.6800	7.9303	114,560	18,330,000	2.8956	0.024999454
3	4.6667	7.9147	81,131	13,010,000	2.8956	0.024944197
4	4.6206	7.9325	83,560	13,370,000	2.8956	0.024999252
5	4.6125	7.9419	89,190	14,270,000	2.8956	0.025000701

Table 5. Summary of parameters estimation (B = 4.4196).

S/N	Latitude (^{0}N)	Longitude (^{0}E)	q (N/m^2)	K_s (N/m^3)	B (m)	S_i (m)
1	4.6767	7.9256	143,380	22,940,000	4.4196	0.025000872
2	4.6800	7.9303	114,560	18,330,000	4.4196	0.024999454
3	4.6667	7.9147	81,131	13,010,000	4.4196	0.024944197
4	4.6206	7.9325	83,560	13,370,000	4.4196	0.024999252
5	4.6125	7.9419	89,190	14,270,000	4.4196	0.025000701

Seismic energy was generated by a source located on the surface and radiates out from the shot point, travelling directly through the upper layer down to and then laterally along higher velocity layers before returning back to the surface. This energy was detected on the surface by the geophones. Two seismic sources; shear wave and compressional wave sources have two sets of geophones each for P-wave and S-wave. A sledge hammer and metal plates were used to generate seismic waves in this refraction study. The P-wave was generated when the hammer was struck vertically on the metal plate while the shear wave was generated when the hammer was struck horizontally on the metal plate. The generated energy penetrated into the subsurface and refracted off at various interfaces corresponding to geological boundaries and consequently returned to the surface at a later time to be picked up by the geophones. The seismic wave received by the geophones was converted into electrical pulse and were amplified. This plot was copied out from the seismograph from which the arrival times were picked using IX Refrax

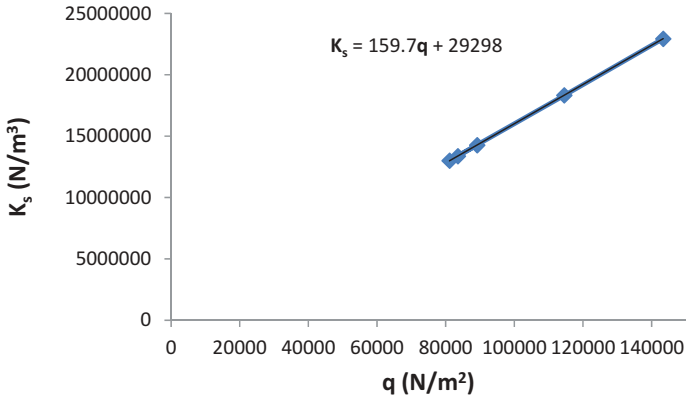

Figure 6. A plot of subgrade coefficient versus bearing pressure.

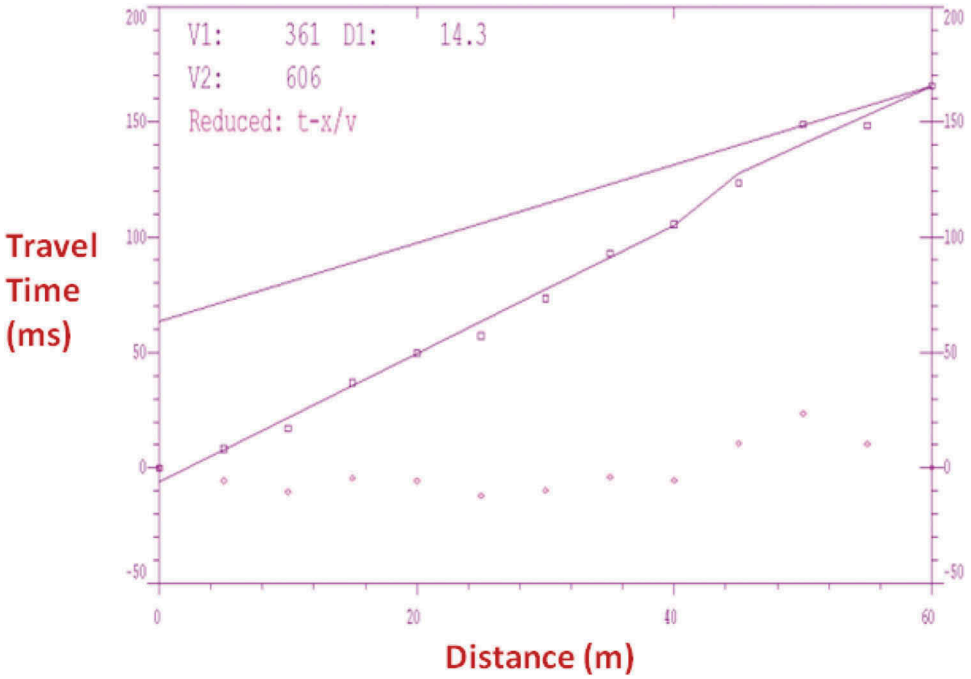

Figure 7. T-X plot of P wave forward data (Latitude 4.6767°N and Longitude 7.9256°E).

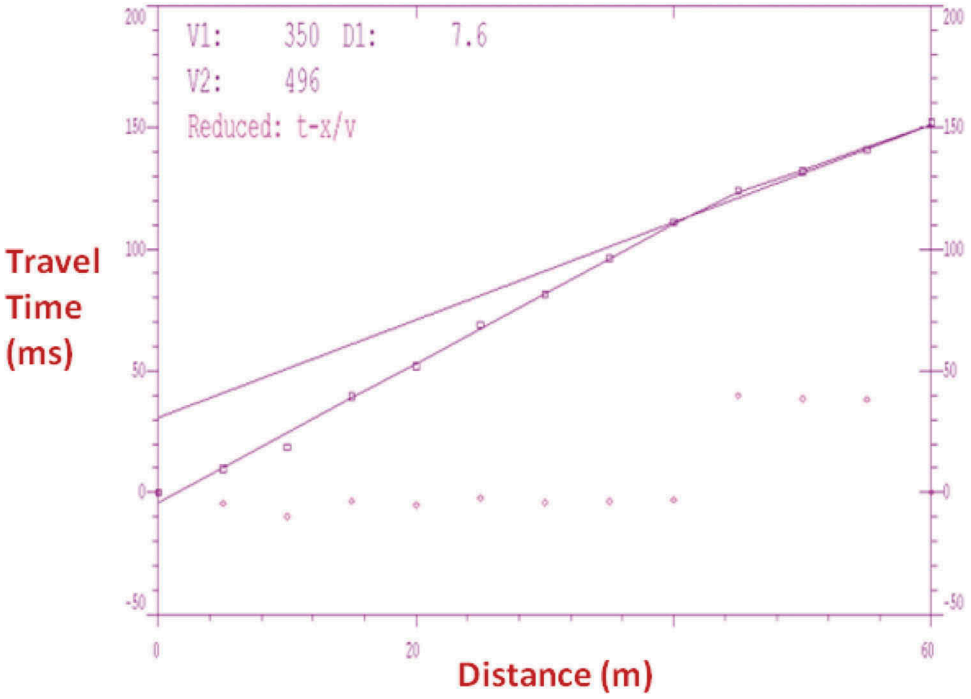

Figure 8. T-X plot of P wave reverse data (Latitude 4.6767°N and Longitude 7.9256°E).

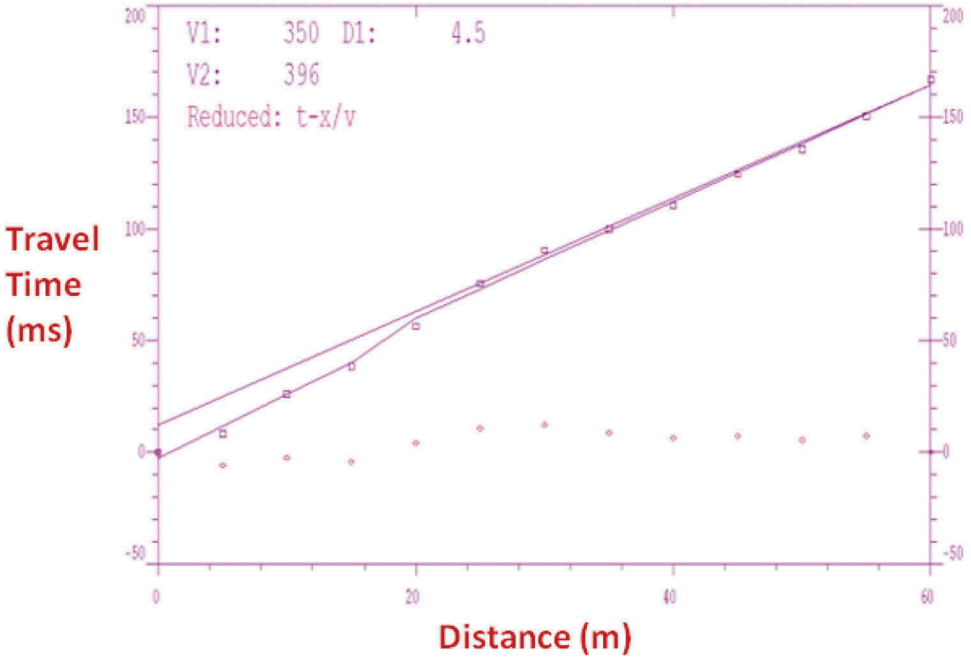

Figure 9. T-X plot of S wave forward data (Latitude 4.6767°N and Longitude 7.9256°E).

and Pickwin softwares and plotted as T-X graph showing two velocity layers. A total of two spreads at different locations were taken. The final process was calculating the velocity of P and S waves and the thickness of each layer in the site based on the intercept time graphic data. The final result interpretation is displayed using the Generalised Reciprocal Method (GRM). The models are presented in Figures 7–24.

The data processing technique of the seismic refraction method is explained schematically in Figure 5. The analogue data of the seismic wave propagation are directly resulted from the field measurement equipment. The seismograph box acquisition unit transferred the analogue data into the digital data. The important information of the digital data for the seismic refraction method is the first arrival time information of P and S waves which propagate to the geophones.

4. Result, data analysis and discussion

The results of the T-X plot of P wave forward and reverse data; S wave forward and reverse data are

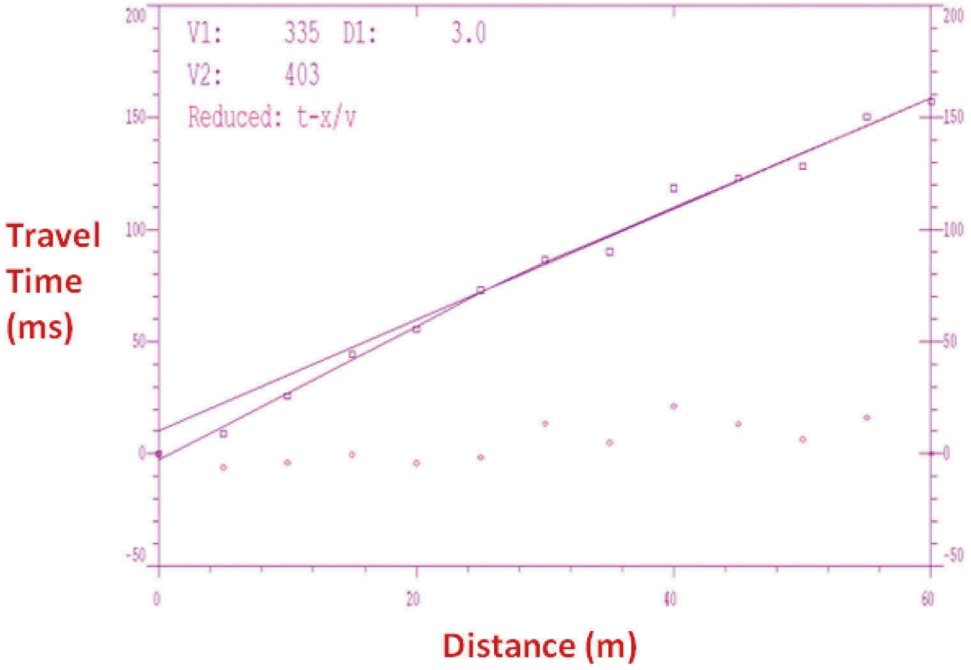

Figure 10. T-X plot of S wave reverse data (Latitude 4.6767°N and Longitude 7.9256°E).

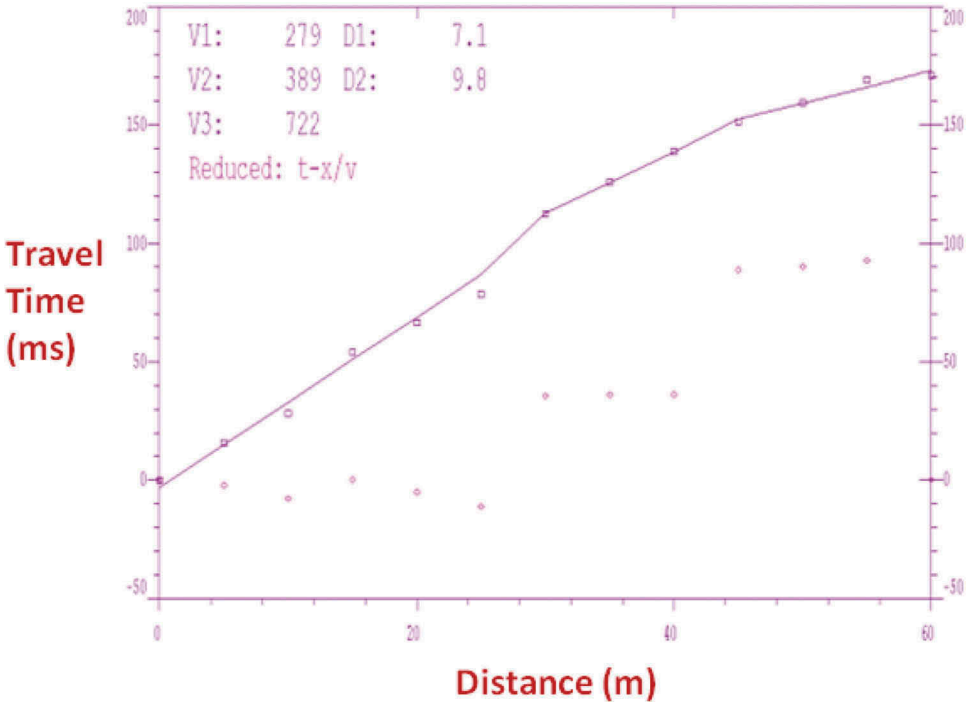

Figure 11. T-X plot of P wave forward data (Latitude 4.6800°N and Longitude 7.9303°E).

presented in Figures 7–24. These graphs provided useful information, by enabling the determination of layer velocities (the inverse of each segment of the graph) of the overburden layers, which are cardinal in this study. In Figures 15 and 16, the section of the layer that the wave energy refracted through is also imaged. The results of the estimated parameters at their respective locations for B = 0.524, 1.3716, 2.8956, 4.4196 m are indicated in Tables 2–5. Subgrade coefficient relates linearly with bearing pressure as provided in (Figure 6).

During data acquisition, individual shot records were presented as variable area wiggle traces displaying travel time against distance (x). These allowed an initial calculation of overburden and refractor apparent velocities and provided an import check on the value of the data. The acquisition wiggle traces were used to display the data during picking of the first arrivals for each geophone position and shot. The processed data were presented as series of time-distance graphs (Figures 7–24) where compressional and shear wave velocities for each layer were

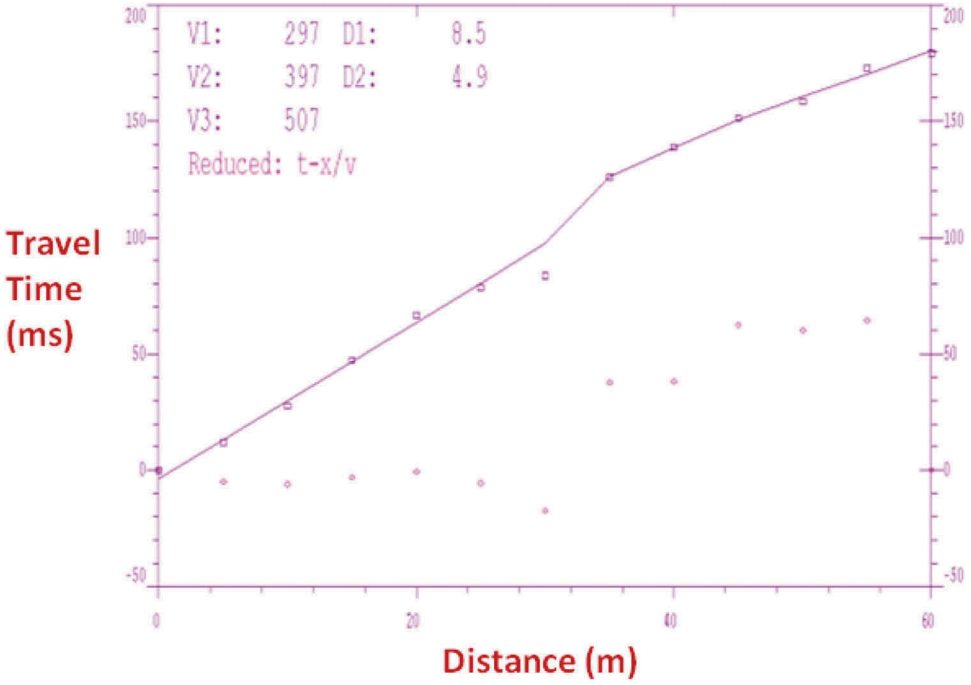

Figure 12. T-X plot of P wave reverse data (Latitude 4.6800°N and Longitude 7.9303°E).

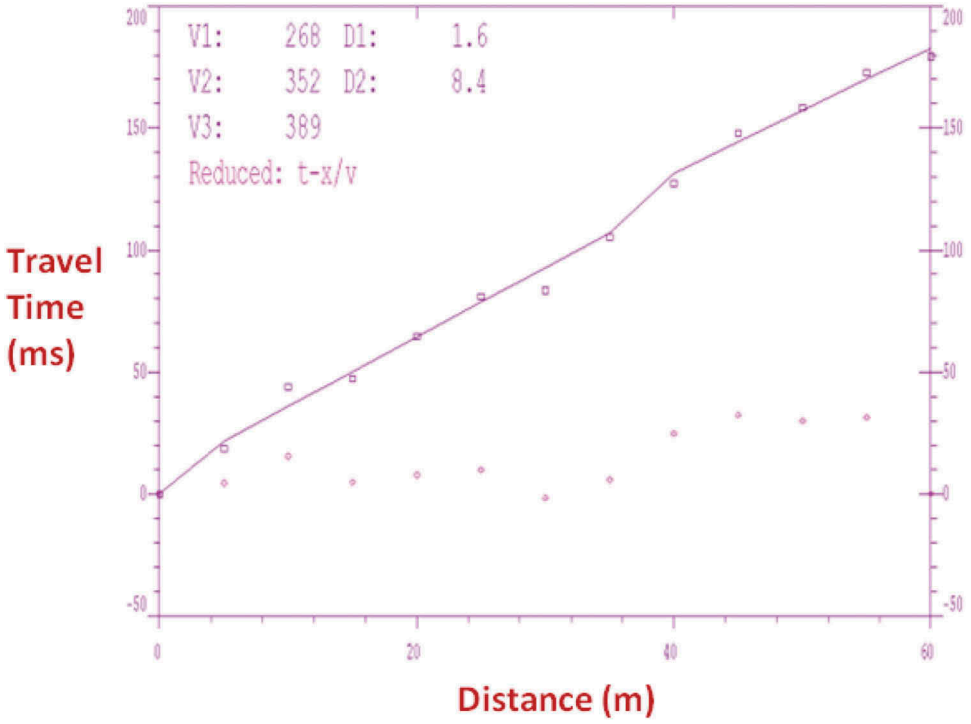

Figure 13. T-X plot of S wave forward data (Latitude 4.6800°N and Longitude 7.9303°E).

obtained leading to the evaluation of V_P/V_S ratios, Poisson's ratio, Shear Modulus, Young's Modulus, Bulk Modulus and other parameters. These parameters relate with bearing pressure.

The decease of shear travel time (increase of V_s) is due to the decrease of density and the absorption of deformation by free gas in pores. The increase of compressional travel time (decrease of V_P) is due to the decrease of the bulk modulus of reservoir rocks, which compensate for the decrease of rock density. S wave does not propagate through a fluid or gas because a fluid (gases) cannot transmit shear stress hen its low values correspond to wave speed in loose, unconsolidated sediment.

Tables 2–5 show the result of immediate settlement of footings. These were computed using Equation (3). The values are the same (approximately 0.025 m) for all locations in the area. Settlement shows vertically

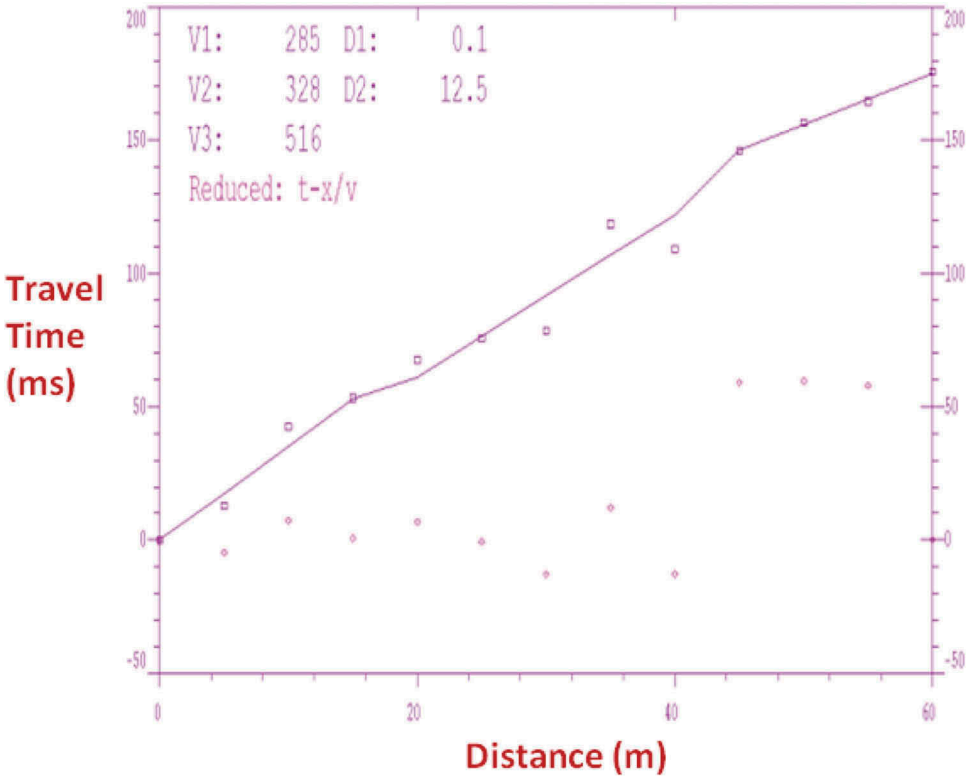

Figure 14. T-X plot of S wave reverse data (Latitude 4.6800°N and Longitude 7.9303°E).

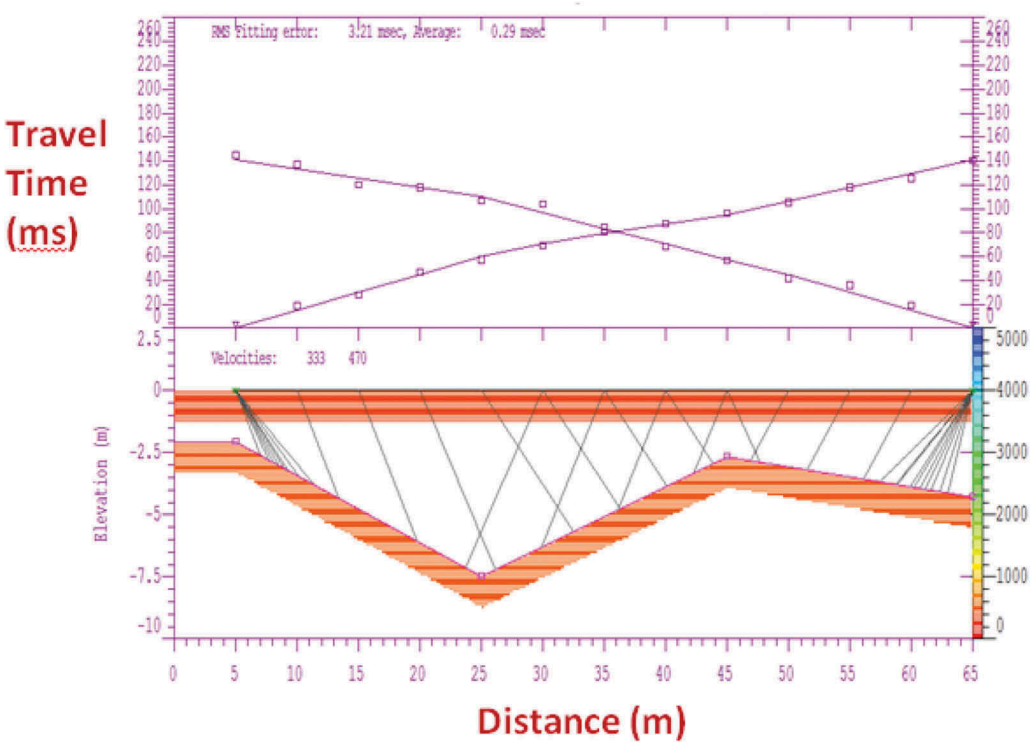

Figure 15. T-X plot of P wave forward and reverse data (Latitude 4.6667°N and Longitude 7.9147°E).

downward movement of structure due to compression of underlying soil of increased load. The soil is cohesionless. Cohesionless soils are free flowing when dry or completely saturated. This soil under investigation is loose sandy material. It does not exhibit plasticity (particles do not readily stick to each other). The implication of the results computed in Tables 2–5, is that with 1694 psf (or 81,131 Pa) $\leq q \leq$ 29934 psf (or 143,380 Pa) range, the class of materials in the area (first layer) falls under row five and row six, column one of Internationl Residential Code (2006) in Table 1. The allowable soil bearing capacity is the maximum pressure that can be

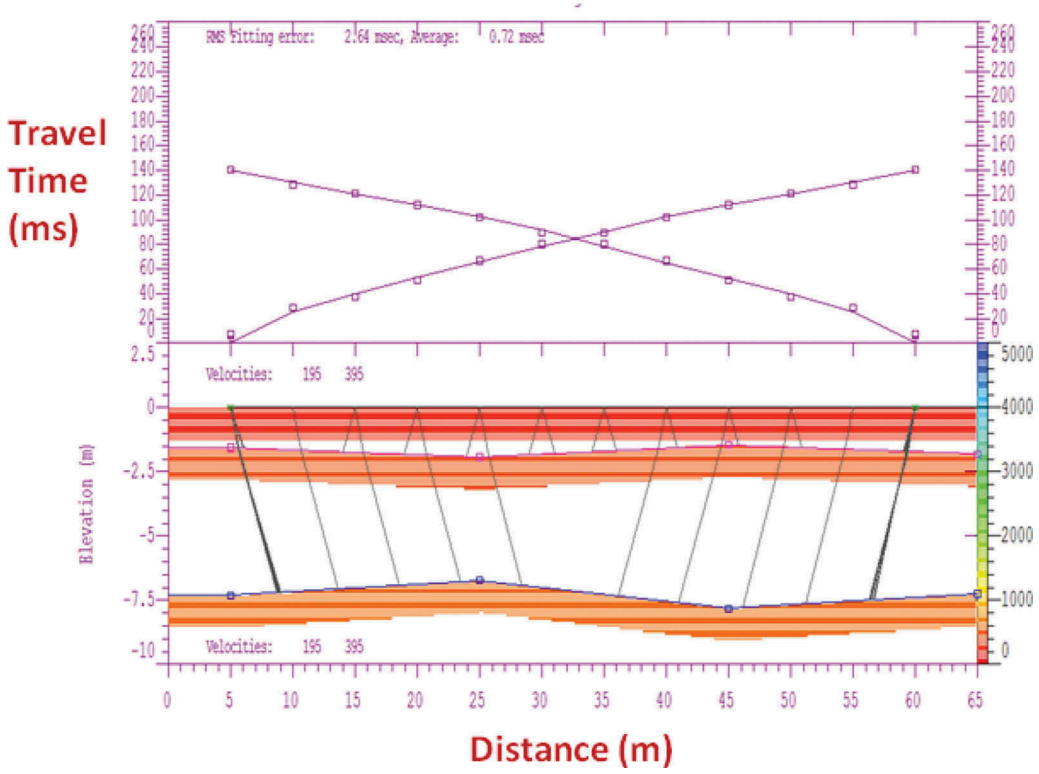

Figure 16. T-X plot of S wave forward and reverse data (Latitude 4.6667°N and Longitude 7.9147°E).

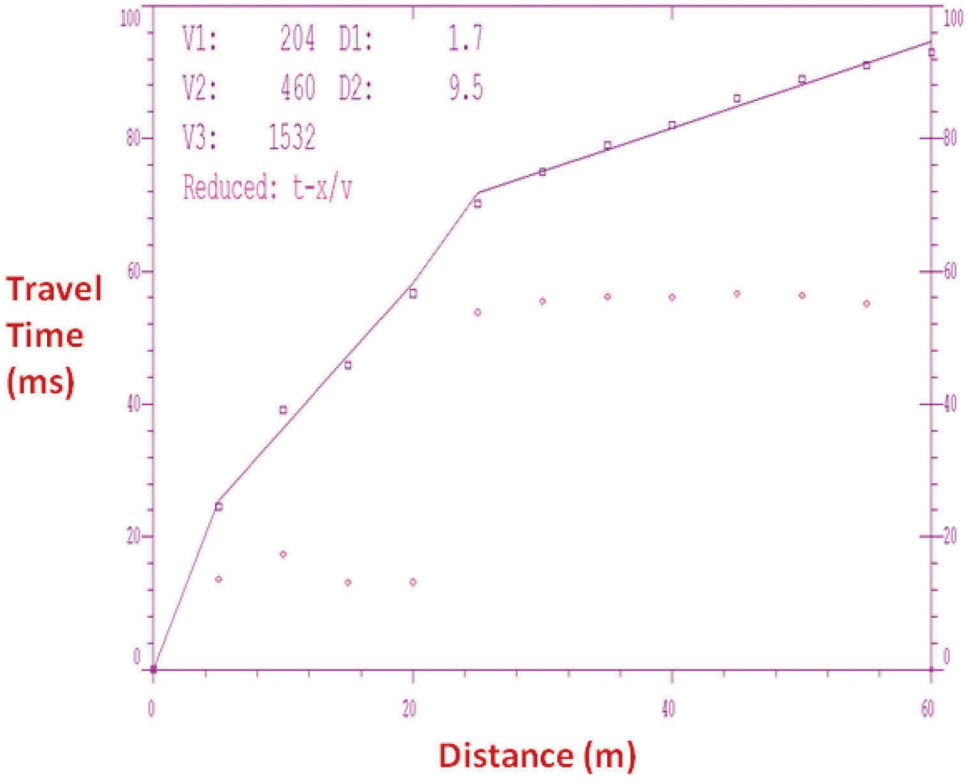

Figure 17. T-X plot of P wave forward data (Latitude 4.6206°N and Longitude 7.9325°E).

permitted on foundation soil with adequate safety against soil rupture or settlement is within the above boundary limit as this will not allow or lead to soil rupture or increase in immediate settlement. The width of the footing will not affect the immediate settlement. The plot of Subgrade coefficient versus Bearing pressure shows how strongly correlated the two parameters are. The plot of Subgrade coefficient versus bearing pressure gives a linear function with a threshold subgrade coefficient of 29,298 Nm^{-3}. The gradient of the relation reflects

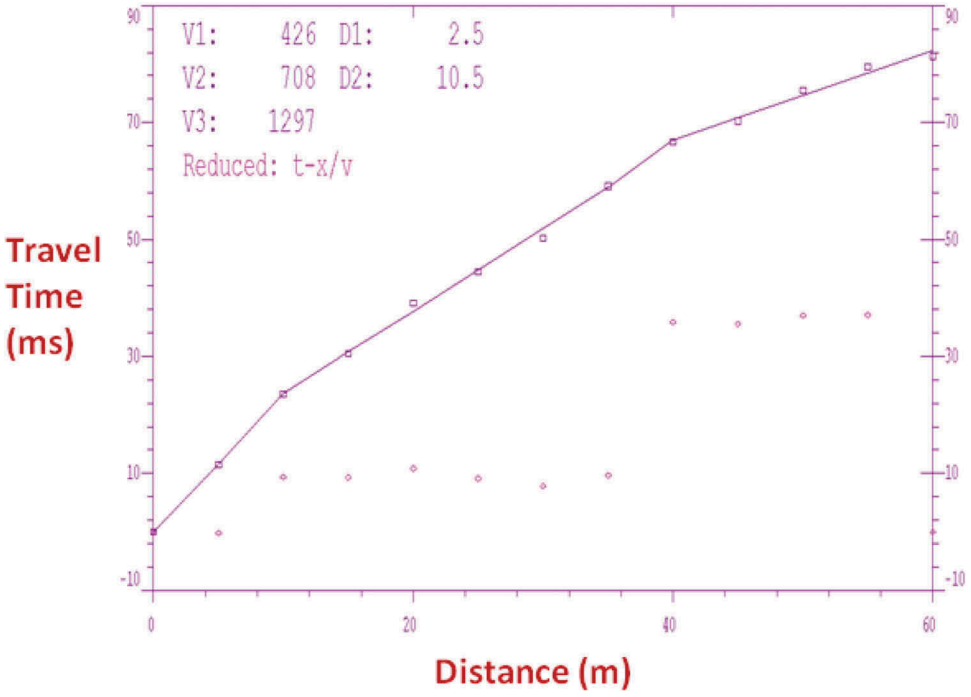

Figure 18. T-X plot of P wave reverse data (Latitude 4.6206°N and Longitude 7.9325°E).

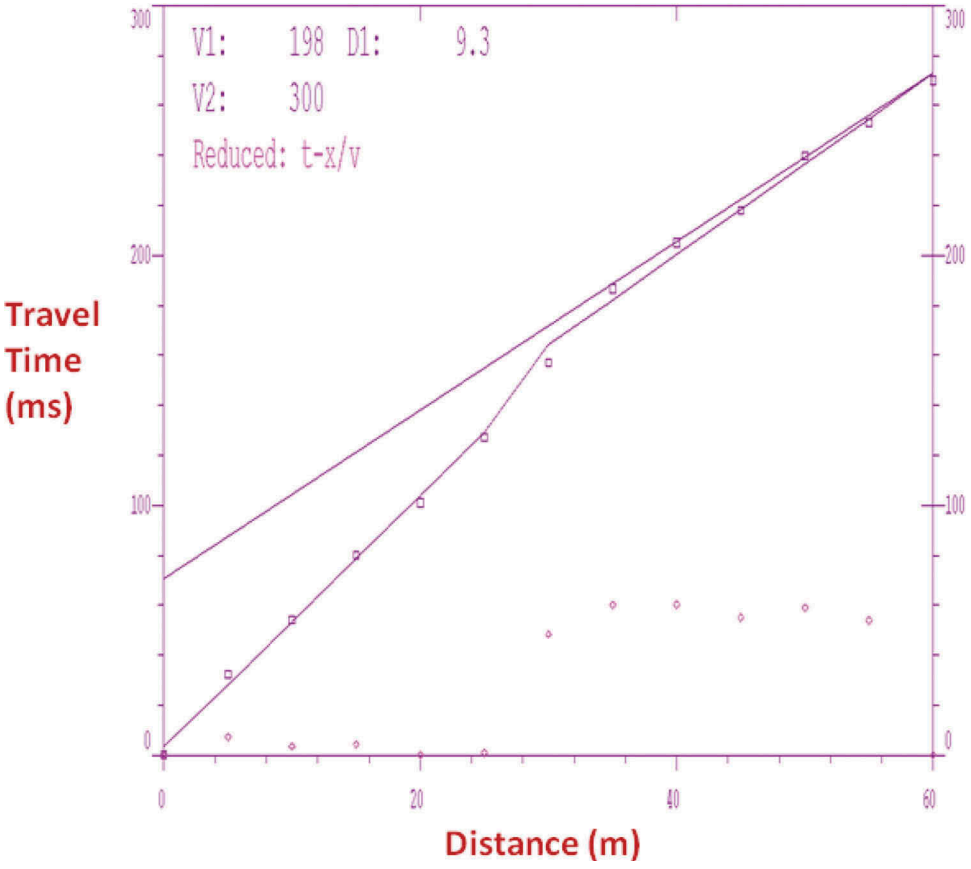

Figure 19. T-X plot of S wave forward data (Latitude 4.6206°N and Longitude 7.9325°E).

the descent of footing under load per metre. Also, from Figure 6, K_s = 159.7q + 29,298; $q = 0.00625K_s$; The range of q is from 81,131 Pa to 6,159,810 Pa for $S_i = 0.025m$; $B <$ 20 ft.

4.1. Summary

From the result, immediate settlement of footing was assessed using seismic refraction data obtained from five different locations in Eket Local Government

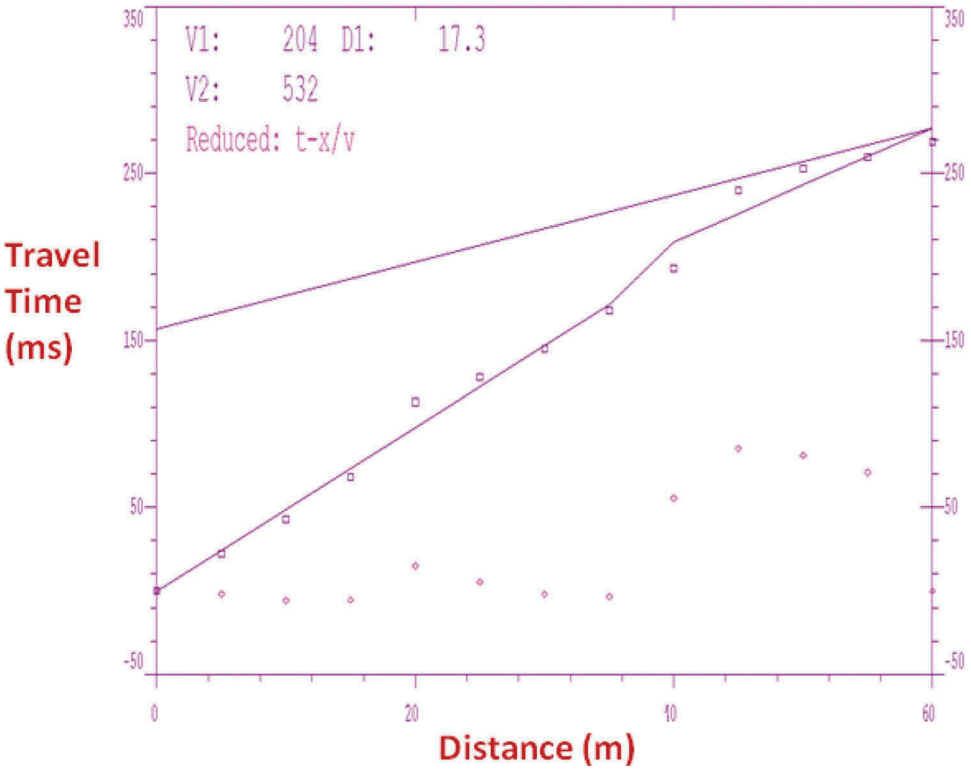

Figure 20. T-X plot of S wave reverse data (Latitude 4.6206°N and Longitude 7.9325°E).

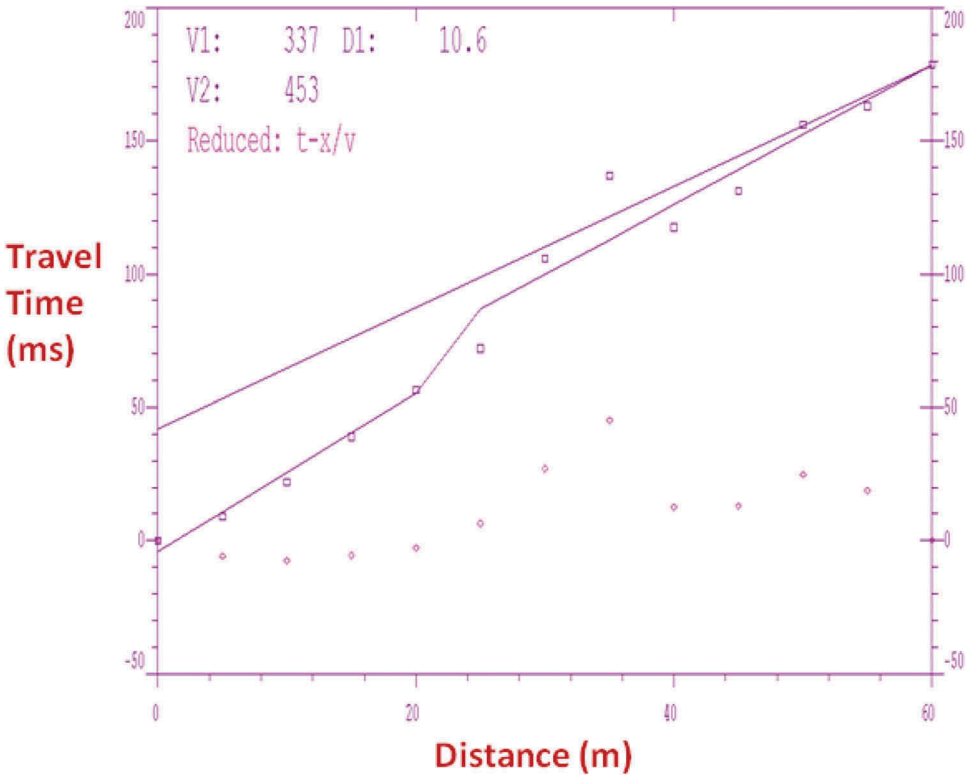

Figure 21. T-X plot of P wave forward data (Latitude 4.6125°N and Longitude 7.9419°E).

Area. The results show that immediate settlement of footing is approximately 0.025 m in all the locations. This was determined at width B $<$ 20 ft (6.096 m). The boundary condition (limit) for bearing pressure in the area by this study falls within the range of 1694 psf (or 81,131 Pa) $\leq q \leq$ 29934 psf (or 143,380 Pa). The class of materials in the area (first layer) falls under row five and row six, column one of Internationl Residential Code (2006). The study reveals that the area has a threshold subgrade coefficient of 29,298 Nm^{-3} while

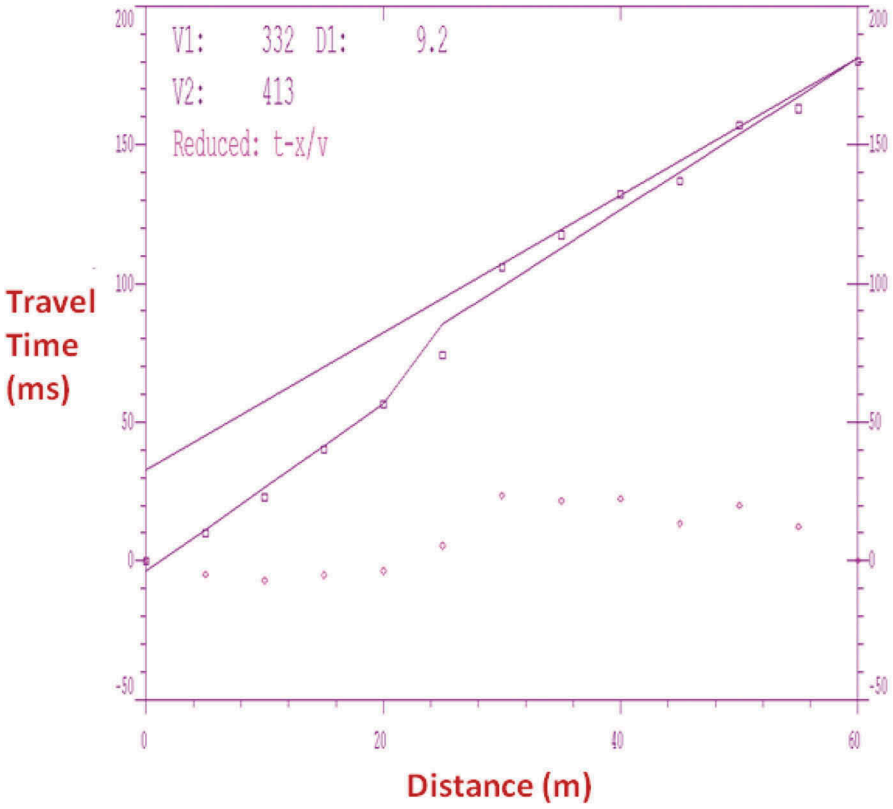

Figure 22. T-X plot of P wave reverse data (Latitude 4.6125°N and Longitude 7.9419°E).

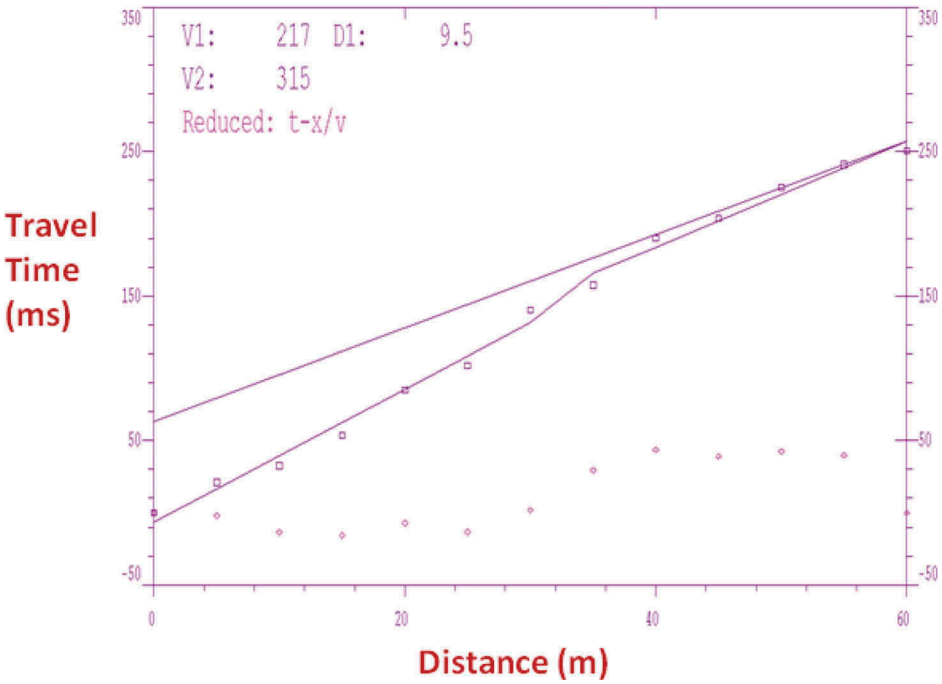

Figure 23. T-X plot of S wave forward data (Latitude 4.6125°N and Longitude 7.9419°E).

the descent of footing under load per metre is 159.7. These parameters further characterise the foundation under load in the study area.

4.2. Conclusion

We have carried out seismic refraction survey in Eket, Nigeria to obtain elastic parameters, aided us achieve our goal since these parameters relate with allowable bearing pressure. Based on the analysis of data and interpretation, seismic refraction study has verified to be very useful in footing studies. This can be seen in its ability to classify the anisotropic materials and artificial top soil constituents that will not support sustainable ground work construction. The decease of shear travel time (increase

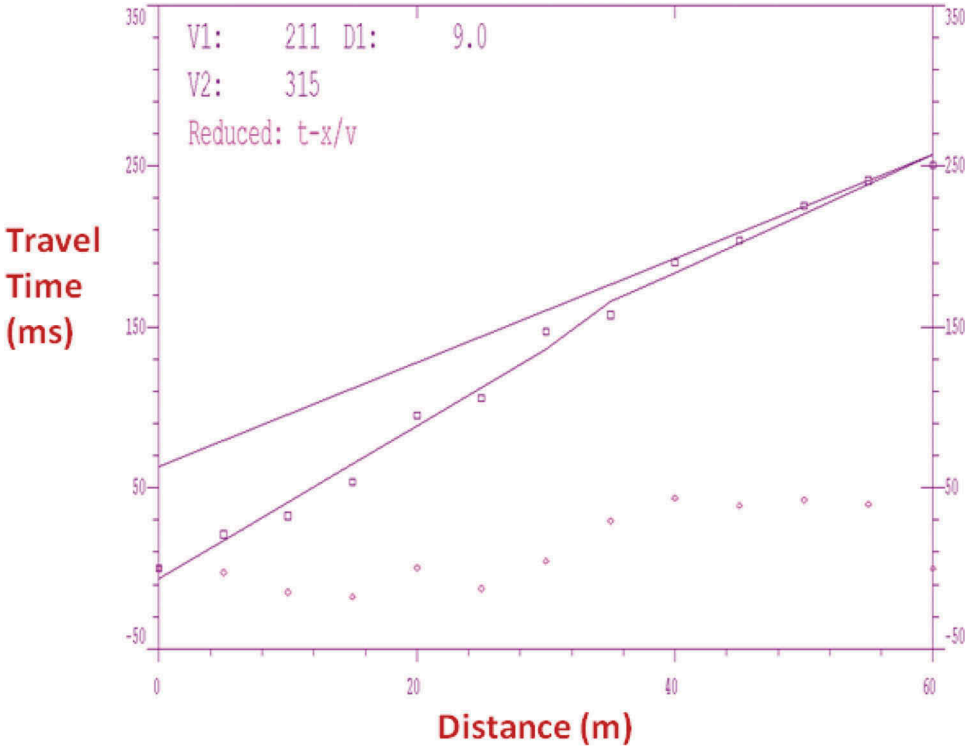

Figure 24. T-X plot of S wave reverse data (Latitude 4.6125°N and Longitude 7.9419°E).

of V_s) may be due to the decrease in density of foundation formation. The increase of compressional travel time (decrease of V_P) is due to the decrease in the bulk modulus of rocks, which compensates the decrease of rock density.

Naval Facilities (NAVFAC) method of determining immediate settlement of footings was employed to predict immediate settlement of footings in the south-eastern part of Niger Delta region. Our findings show that there is no significant change in the immediate settlement as the width of the first layer foundation gradually increases. The boundary condition (limit) for bearing pressure in the area varies as 1694 psf (or 81,131 Pa) $\leq q \leq$ 29934 psf (or 143,380 Pa). The class of materials in the area (first layer) falls under row five and row six, column one of Internationl Residential Code (2006). Subgrade coefficient and Bearing pressure are strongly related.

Acknowledgements

The authors greatly acknowledge the anonymous reviewers and the editor for providing the useful information that has upgraded the quality of this paper.

Disclosure statement

No potential conflict of interest was reported by the authors.

Funding

This paper was funded by authors;UNIUYO [NIL].

ORCID

Joseph Gordian Atat http://orcid.org/0000-0002-2861-3736
Anthonia Gordian Atat http://orcid.org/0000-0002-8529-5826

References

Arora KR. 2009. Soil mechanics and foundation engineering (Geotechnical engineering). Delhi: Standard Publishers Distributors.

Atat JG, Akpabio IO, George NJ. 2013. Allowable bearing capacity for shallow foundation in Eket local government area, Akwa Ibom state, Southern Nigeria. Int J Geosci. 4 (10):1491–1500. doi:10.4236/ijg.2013.410146.

Birid KC, Chachar RS. 2016. Measured and predicted settlement of shallow foundations on cohesionless soil. Indian Geotechnical Conference; December 15–17; Chennai (India): IIT Madras.

Budhu M, Al-Karni A. 1993. Seismic bearing capacity of soils. Geotechnique. 43(1):181–187. doi:10.1680/geot.1993.43.1.181.

Dormieux L, Pecker A. 1995. Seismic bearing capacity of foundation on cohesionless soil. J Geotech Eng. 121 (3):300–303. doi:10.1007/s11771-007-0139-4.

Fumal TE, Tinsley JC. 1985. Mapping shear wave velocities of near-surface geological materials. In: Ziony JI, editor. Predicting area limits of earthquake induced

land sliding: in evaluation of earthquake hazards in the Los Angeles region – an earth science prospective. Vol. 1360. United States Geological Survey Paper; p. 127–150.

Internationl Residential Code. 2006. New Jersey Edition.

Kumar J, Kumar N. 2003. Seismic bearing of rough footings on slopes using limit equilibrium. Geotechnique. 53 (3):363–369. doi:10.1680/geot.2003.53.3.363.

NAVFAC. 1982. Soil mechanics. Department of the Army Design Manuel 7.1.

NAVFAC. 1997. Soil dynamics and special design aspects-superseding NAVFAC DM – 7.3, 1983. Department of Defense Handwork; pp 1–157.

Paolucci R, Pecker A. 1997. Seismic bearing capacity of shallow strip foundations on dry soils. Soils Found. 37 (3):95–105. doi:10.3208/sandf.37.3_95.

Resin D, Kasktas AS. 2009. Observed and predicted settlement of shallow foundation. 2nd International Conference on New Developments in Soil Mechanics and Geotechnical Engineering; May 28–30; Nicosia (North Cyprus): Near East University.

Richards R, Elms DG, Budhu M. 1993. Seismic bearing of capacity and settlements of foundations. J Geotech Eng. 119(4):662–674. doi:10.1061/(ASCE)0733-9410-(1993)119:4(662).

Sarma SK, Lossifelis IS. 1990. Seismic bearing capacity factors of shallow strip footings. Geotechnique. 40 (2):265–273. doi:10.1680/geot.1990.40.2.265.

Scott JH, Lee FT, Carroll RD, Robinson CS. 1968. The relationship of geophysical measurements to engineering and construction parameters in the straight, creek tunnel pilot boring colorado. Int J Rock Mech Min. 5(1):1–30. doi:10.1016/0148-9062(68)90020-X.

Soubra AH. 1997. Seismic bearing capacity of shallow strip footings in seismic conditions. Proc Inst Civil Eng – Geotech Eng. 125(4):230–241. doi:10.1680/igeng.1997.29659.

Terzaghi K, Peck RB. 1967. Soil mechanics in engineering practice. 2nd ed. London: John Wiley and Sons.

Terzaghi K, Peck RB, Mesri G. 1996. Soil mechanics in engineering practice. 3rd ed. New York: John Wiley and Sons.

Tezcan S, Ozdemir Z, Keceli A. 2009. Seismic technique to determine allowable bearing pressure for shallow foundations in soils and rocks. Acta Geophys. 57(2):1–14. doi:10.2478/S11600-008-0077-z.

Tezcan SS, Keceli A, Ozdemir Z. 2006. Allowable bearing capacity of shallow foundation based on shear wave velocity. J Geotech Geol Eng. 24(1):203–218. doi:10.1007/s10706-004-1748-4.